

ORIGINAL PAPERS

Apoptosis related to telomere instability and cell cycle alterations in human glioma cells treated by new highly selective G-quadruplex ligands

Gaëlle Pennarun¹, Christine Granotier¹, Laurent R Gauthier¹, Dennis Gomez², Françoise Hoffschir¹, Eliane Mandine³, Jean-François Riou², Jean-Louis Mergny⁴, Patrick Mailliet³ and François D Boussin^{*1}

¹Laboratoire de Radiopathologie, DSV/IDRR, CEA, 18 route du Panorama, 92265 Fontenay-aux-Roses, France; ²Laboratoire d'Onco-Pharmacologie, JE 2428, Université de Reims Champagne-Ardenne, 51096 Reims, France; ³Aventis Pharma SA, Centre de Recherche de Paris, 94403 Vitry-sur-Seine, France; ⁴Laboratoire de Biophysique, INSERM U565, CNRS UMR 5153, Muséum National d'Histoire Naturelle USM 503, 75005 Paris, France

Telomerase represents a relevant target for cancer therapy. Molecules able to stabilize the G-quadruplex (G4), a structure adopted by the 3'-overhang of telomeres, are thought to inhibit telomerase by blocking its access to telomeres. We investigated the cellular effects of four new 2,6-pyridine-dicarboxamide derivatives displaying strong selectivity for G4 structures and strong inhibition of telomerase in *in vitro* assays. These compounds inhibited cell proliferation at very low concentrations and then induced a massive apoptosis within a few days in a dose-dependent manner in cultures of three telomerase-positive glioma cell lines, T98G, CB193 and U118-MG. They had also antiproliferative effects in SAOS-2, a cell line in which telomere maintenance involves an alternative lengthening of telomeres (ALT) mechanism. We show that apoptosis was preceded by multiple alterations of the cell cycle: activation of S-phase checkpoints, dramatic increase of metaphase duration and cytokinesis defects. These effects were not associated with telomere shortening, but they were directly related to telomere instability involving telomere end fusion and anaphase bridge formation. Pyridine-based G-quadruplex ligands are therefore promising agents for the treatment of various tumors including malignant gliomas.

Oncogene (2005) 24, 2917–2928. doi:10.1038/sj.onc.1208468
Published online 14 February 2005

Keywords: glioma; anticancer agent; G-quadruplex ligands; apoptosis

Introduction

In most somatic cells, telomeres – the nucleoprotein structures at the end of eukaryotic chromosomes – progressively shorten with successive cell divisions until they reach a particular state in which replicative

senescence is triggered, leading to cell-cycle arrest (for a review, see McEachern *et al.*, 2000). Telomeres are maintained by telomerase, a specific reverse transcriptase. The catalytic subunit of this enzyme, hTERT, uses its RNA subunit (hTR) as a matrix for adding TTAGGG repeats to the ends of chromosomes. Telomerase gene expression is repressed in most somatic cells, although limited expression associated with the S phase has been observed in normal cycling cells (Masutomi *et al.*, 2003). In contrast, it is reactivated in the vast majority of tumors (90%). Telomerase is thought to render cancer cells capable of unlimited proliferation by maintaining and protecting telomeres (Shay and Bacchetti, 1997; Chan and Blackburn, 2002). Telomerase is therefore considered to be a relevant, promising target for the development of new anticancer drugs. However, telomere length may also be maintained in some cancer cells by an alternative lengthening of telomeres (ALT) mechanism based on homologous recombination (Henson *et al.*, 2002).

Several classes of telomerase inhibitors have been developed in recent years (Mergny *et al.*, 2002). These inhibitors include G-quadruplex ligands, which target the telomeres rather than telomerase itself. G-quadruplex ligands are thought to inhibit telomerase activity by stabilizing the folding of the telomeric G-rich single-stranded overhang into a four-stranded DNA structure called the G-quadruplex (Zahler *et al.*, 1991; Neidle and Parkinson, 2003). Some of these ligands have been shown to impair telomerase function in cancer cells, resulting in replicative senescence, which is associated with both telomere shortening and terminal growth arrest (Gowan *et al.*, 2002; Riou *et al.*, 2002; Shammas *et al.*, 2003; Tauchi *et al.*, 2003). Interestingly, as they interact directly with telomeres, and not telomerase, G-quadruplex ligands may also be effective in cancer cells proliferating by ALT-dependent mechanisms (Gowan *et al.*, 2001; Riou *et al.*, 2002; Kim *et al.*, 2003).

Malignant gliomas are the most common primary tumor of the central nervous system and represent the second leading cause of cancer-related deaths in children and young adults. The most frequent form, glioblastoma multiforme, is very aggressive and invasive and is

*Correspondence: F Boussin; E-mail: boussin@cea.fr
Received 11 October 2004; revised 8 December 2004; accepted 20 December 2004; published online 14 February 2005

highly refractory to anticancer treatment. Glioblastoma patients generally survive for less than 18 months after diagnosis, despite treatment by a combination of surgery, radiation therapy and chemotherapy (Holland, 2000). Although much less frequent than telomerase activation in most cancer types, it has been suggested that ALT occurs in almost 25% of glioblastoma multiforme tumors (Hakin-Smith *et al.*, 2003).

In this study, we investigated a new series of 2,6-pyridine-dicarboxamide derivatives, selected *in vitro* on the basis of highly selective interactions with telomeric G-quadruplex (as compared with double-stranded DNA) and for their potent inhibitory effects on telomerase (Mailliet *et al.*, 2003). These new ligands induced a delayed growth arrest followed by massive apoptosis in three telomerase-positive glioma cell lines, T98G, CB193 and U118-MG. These effects were related to multiple alteration of cell cycle progression including activation of S-phase checkpoints, increase of metaphase duration and defects in cytokinesis that appeared directly linked to telomere instability. The pyridine derivatives also had antiproliferative effects on SAOS-2, an ALT cell line. These pyridine-based G-quadruplex ligands provide therefore new opportunities for the development of alternative treatments for malignant gliomas proliferating by telomerase- or ALT-dependent mechanisms.

Results

In vitro properties of new G-quadruplex ligands

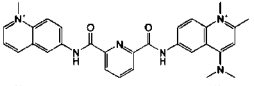
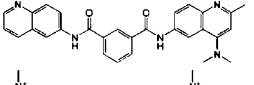
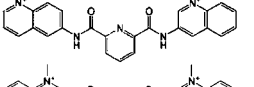
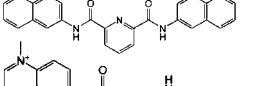
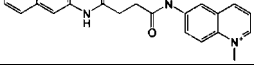
Four new G-quadruplex-interactive telomerase inhibitors (831A, 832A, 307A and 360A) were selected from a series of 2,6-pyridine-dicarboxamide derivatives

(Table 1) on the basis of their potent and selective inhibition of telomerase activity and stabilization of telomeric G-quadruplex DNA (Mailliet *et al.*, 2003). The biochemical affinities and selectivities of these compounds for telomerase inhibition and G-quadruplex stabilization are presented in Table 1. The stabilization of a telomeric G-quadruplex was assessed by G4-FRET. The ΔT_m values obtained for these ligands were $> 20^\circ\text{C}$, indicating strong interactions with four-stranded structures. These new compounds also displayed potent telomerase inhibition with IC_{50} values of 0.22–0.45 μM , associated with a high selectivity ratio (33–150) with respect to Taq polymerase inhibition in the TRAP-G4 assay (Gomez *et al.*, 2002). These ligands also had a much higher affinity for G-quadruplex structures than for other forms of nucleic acids, as demonstrated by equilibrium dialysis experiments and other techniques (Lemarteleur *et al.*, 2004; Mandine *et al.*, in progress; Guittat *et al.*, in progress). Thus, ligands from the 2,6-pyridine-dicarboxamide series reported here are about 10 times more selective than the previously described derivative 115405 from the 2,4,6-triamino-1,3,5 triazine series (Riou *et al.*, 2002). 307A and 360A displayed the best compromise between activity and selectivity *in vitro*. Another dicarboxamide derivative, 979A, which lacks the central pyridine moiety (Table 1) and does not interact with quadruplex structures or inhibit telomerase (at concentrations up to 10 μM), was also selected as a useful negative control for subsequent cellular experiments.

Pyridine derivatives reduced the viability of telomerase-positive glioma and ALT cell lines

We investigated the cellular effects of pyridine derivatives on three telomerase-positive glioma cell lines with

Table 1 *In vitro* properties of the new pyridine derivatives

Name	Pyridines Chemical structure	Telomerase		G-quadruplex	
		TRAP ^a IC_{50} (μM)	Selectivity ^b	Stabilization ^c ΔT_m $^\circ\text{C}$	Selectivity ^d
831A		0.22	70	24.5	35–40
832A		0.45	33	26	> 20
307A		0.3	150	21	> 50–100
360A		0.3	150	21	> 50
979A ^e		> 20		0	

^aMeasured by TRAP-G4 assay (Riou *et al.*, 2002). ^bRatio of IC_{50} against telomerase to IC_{50} against the internal PCR control (Gomez *et al.*, 2002). ^cMeasured by G4 FRET assay (Riou *et al.*, 2002). ^dIndex obtained by alphascreen test (Mandine *et al.*, in preparation). This high-throughput luminescent assay allows measuring the pairing inhibition of a telomere-based oligonucleotide, able to form G4 structure, with its complementary strand. The inhibition of pairing of a closely related oligonucleotide, unable to form any G4, is measured in parallel, thus enabling to evaluate the selectivity of ligands versus B-DNA. ^eInactive compound

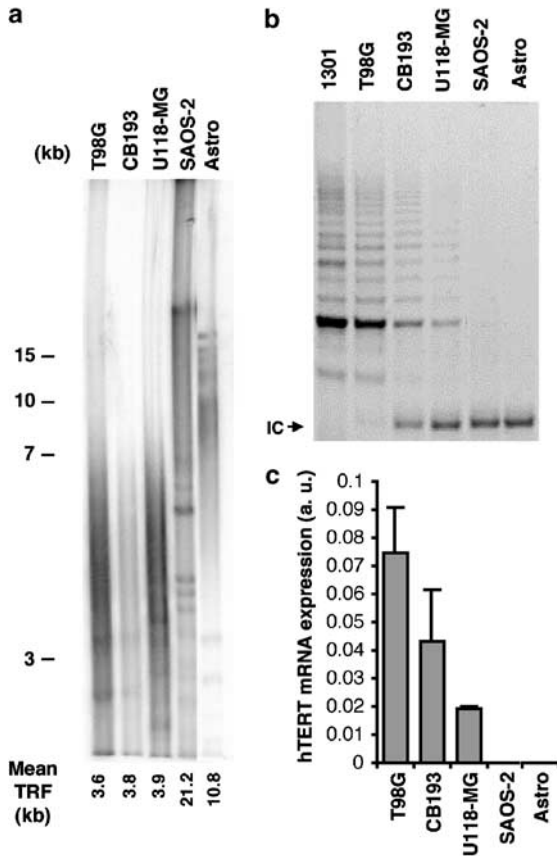


Figure 1 Characterization of telomeres/telomerase status of target cells. (a) Mean TRF length determination. High-molecular weight DNA was digested with *HinfI* and run on a 0.5% agarose gel. The gel was Southern blotted and the blot was hybridized with a ³²P-labeled telomeric probe. (b) TRAP products were analysed by electrophoresis in a 12.5% polyacrylamide gel, stained with ethidium bromide. We used 100 ng of protein extract from each sample in the TRAP assay. High levels of telomerase activity were found in T98G, CB193 and U118-MG malignant glioma cells, whereas the ALT cell line, SAOS-2, displayed no telomerase activity like the normal astrocytes used as telomerase-negative control cells. CEM1301 cells were used as a telomerase-positive control. The arrow indicates the 36 bp internal control (IC) for PCR. The data are representative of two independent experiments. (c) Detection and evaluation of hTERT mRNA levels by semiquantitative real-time RT-PCR. hTERT transcripts were detected in T98G, CB193 and U118-MG glioma cell lines, but not in SAOS-2 cells, or normal astrocytes. hTERT mRNA levels are expressed with respect to those in CEM1301 cells and are normalized with respect to that of 18S rRNA. The data are the means \pm s.d. of two independent experiments

short telomeres (mean telomere restriction fragment (TRF) lengths lower than 4 Kb): T98G, CB193 and U118-MG, and on a primary culture of normal astrocytes (telomerase negative and with a mean TRF length around 10 kb) (Figure 1a and b). The telomerase status of the cell lines was further confirmed by semiquantitative real-time PCR (Figure 1c), showing that glioma cell lines expressed large amounts of hTERT mRNAs, encoding the catalytic subunit of telomerase, whereas these mRNAs were undetectable in normal astrocytes. Although it has been suggested that ALT

occurs in a significant proportion of glioma patients (Hakin-Smith *et al.*, 2003), no glioblastoma cell line displaying ALT has yet been described. We therefore also investigated the possible effects of the G-quadruplex ligands on this particular type of glioma, using as model a previously described ALT osteosarcoma cell line: SAOS-2 (Bryan *et al.*, 1997). This typical ALT cell line lacks telomerase activity and hTERT mRNAs and has highly heterogeneous telomere lengths, with some very long telomeres exceeding 20 kb (Figure 1).

We first assessed the cellular effects of the G-quadruplex ligands using the WST-1 assay in short-term cultures (3 and 7 days). This assay allowed us to measure the results of their effects on cell proliferation and cell death. We observed no cellular effect in any of the cell types after 72 h of treatment with any of the pyridine derivatives for concentrations up to 20 μ M. In contrast, the triazine derivative 115405 dramatically decreased the cell viability in all cell cultures, causing a massive cell death with IC₅₀ between 0.4 and 0.9 \pm 0.3 μ M. The rapid kinetic of the induction of cell death by this compound, which is not selective for G-quadruplex structures in *in vitro* assays, is consistent with published data (Riou *et al.*, 2002).

After 7 days of treatment (Table 2), no effect of G-quadruplex ligands was found in primary astrocyte cultures, for concentrations up to 20 μ M, except a reduced effect of 360A (IC₅₀ of 17.4 μ M). However, we showed using WST-1 assay that the pyridine derivatives 307A, 360A and 832A significantly decreased cell viability and/or cell proliferation in the telomerase-positive glioma cell lines T98G and CB193, with IC₅₀ between 2.6 and 13.3 μ M, whereas U118-MG cells were sensitive only to 360A, with an IC₅₀ of 8.4 μ M. The ALT cell line, SAOS-2, were sensitive to 307A and 832A, with IC₅₀ between 5.7 and 6.9 μ M, consistent with previous reports showing that compounds interacting with G-quadruplex structures inhibit proliferation in cells maintaining telomeres by the ALT mechanism (Gowan *et al.*, 2001; Riou *et al.*, 2002; Kim *et al.*, 2003).

The inactive pyridine derivative 979A had no effect on any of the cell types tested, suggesting that the cellular effects of G-quadruplex ligands were related to the selective binding to and stabilization of the G-quadruplex.

Table 2 Viability assay on glioma cell lines, an ALT cell line and primary astrocyte cultures treated for 7 days with pyridine derivatives

Cell type	IC ₅₀ (μ M) ^a			
	307A	360A	832A	979A
T98G	2.6 \pm 0.5	4.8 \pm 1.1	3.3 \pm 0.2	> 20
CB193	6.9 \pm 1.3	3.9 \pm 0.4	13.3 \pm 2.6	> 20
U118-MG	> 20	8.4 \pm 0.5	> 20	> 20
SAOS-2	5.7 \pm 0.9	> 15	6.9 \pm 0.8	> 20
Primary astrocytes	> 20	17.4 \pm 1.2	> 20	> 20

^aIC₅₀ values obtained using WST-1 assay after 7 days of treatment. Results are means of triplicates (\pm s.d.)

G-quadruplex ligands reduced the rate of population doubling and induced cell death in telomerase-positive glioma and ALT cell lines

We further characterized the biological effects of pyridine derivatives by assessing the effects of treatments on population doublings in long-term cultures (Figure 2). T98G cells were the most sensitive of the three glioma cell lines. Indeed, concentrations of 307A of 0.1–5 μM decreased the rate of cell proliferation in a dose-dependent manner, and this decrease was detectable after 1 week of treatment (Figure 2a). This decrease was followed by complete growth arrest within 2 weeks, associated with massive cell death, as shown by the apparent decrease in PD number between two seedings. Light microscopy on day 13 (Figure 2b) revealed a large decrease in cell density and morphological changes typical of differentiated astrocytes: ramified cells with an increase in cytoplasmic volume, in a significant proportion of cells. A similar pattern of growth arrest and delayed cell death of T98G cells was obtained with the pyridine derivatives 831A, 832A and 360A (data not shown).

In U118-MG cultures, we also observed dose-dependent growth arrest followed by massive cell death within 3 weeks of treatment with 1 or 5 μM 307A (Figure 2a). CB193 cells appeared to be significantly less sensitive (Figure 2a). Indeed, 1 μM 307A had no effect on CB193 cell proliferation for up to 40 days of treatment. However, the treatment of CB193 cells with 5 μM 307A decreased the population-doubling rate within 7 days and led to massive cell death within 2 weeks, resulting in a large decrease in cell density in the culture flasks and changes in cell morphology, with the cells becoming enlarged and changing shape (Figure 2b).

The ALT cell line SAOS-2 was sensitive to the long-term effects of 307A (Figure 2a). 307A (5 μM) abolished cell proliferation and induced cell death within 3 weeks. However, 1 μM 307A induced only a slight inhibition of SAOS-2 cell growth.

Finally, CB193 cultures were unaffected by treatment with 1 and 5 μM of the control, inactive pyridine derivative 979A, and only a slight decrease in population-doubling rate, with no increase in the rate of cell death observed in T98G cultures treated with 5 μM 979A (Figure 2c). Thus, active pyridine derivatives had specific effects related to their G-quadruplex-binding properties. Conversely, the decrease in cell growth rate induced by 979A in T98G cells may reflect nonspecific cellular events. This inactive compound, which is not selective for the G4-structure, may bind elsewhere in the genomic DNA and disturb cellular functions such as DNA replication or gene transcription.

Inhibition of cell cycle progression and induction of apoptosis in CB193 and T98G glioma cells

We detected no SA- β -galactosidase-positive cells in T98G or CB193 cultures treated with the pyridine derivatives, indicating that these compounds did not

induce a senescence program in these cell lines (data not shown).

Cellular DNA content determination by flow cytometry showed that the treatment of T98G with 1 μM 307A induced a marked decrease in the percentage of cells at the G0/G1 phase and dramatically increased the percentage of cells in S phase (Figure 3a). After 7 days of treatment (thus after more than three population doublings, see Figure 2a), 32% of cells were in S phase compared to 21% in untreated control. After 9 days, they were more than 55%, demonstrating that pyridine derivative treatment resulted in a block in S-phase progression.

After 12 days, the dramatic increase in the percentage of cells in sub-G1 phase indicated the induction by 307A of a massive apoptosis (Figure 3a). This was further confirmed by the detection of more than 20% TUNEL-positive cells (Figure 3b).

CB193 cultures treated with 5 μM 307A displayed a similar growth arrest in S phase, followed by massive apoptosis, as shown by the large increase in the percentages of: (1) sub-G1 fraction cells, (2) TUNEL-positive cells (20.6% on day 11 and 39% on day 14) and (3) cells containing cleaved caspase-3 (21.9% on day 11 and 35.2% on day 14) (Figure 4).

The compound also induced apoptosis in SAOS-2 cultures as shown by sub-G1 quantification (Figure 5). However, apoptotic induction was associated with a moderate increase of the fractions of cells in S and G2/M phases (Figure 5), suggesting that the compound triggers different pathways in these ALT cells compared to glioma cell lines.

Finally, time-lapse video live-cell imaging showed that, after 7 days of treatment, 1 μM 307A altered cell cycle progression in T98G cultures not only at the S phase but also led to a dramatic increase of metaphase duration and major cytokinesis alterations (Figure 6). These observations indicate thus that the G-quadruplex ligands have delayed pleiotropic actions on cell cycle progression.

Telomeric instability in cultures treated with pyridine derivatives

We detected no significant change in mean TRF lengths in cultures of T98G cells after 13 days of treatment with 979A or 307A compared to DMSO controls (Figure 7a) and in cultures of CB193 cells after 13 days of treatment with 5 μM 307A (Figure 7b). The telomeric 3'-overhang has been shown to be a key component of telomere structure (Stewart *et al.*, 2003). We have thus examined the effect of the ligands on the telomeric G-overhang by using a non-denaturing hybridization technique (Cimino-Reale *et al.*, 2001; Gomez *et al.*, 2003). Continuous treatment of T98G cells with 1 μM 307A led to a slight, but significant decrease of the G-overhang signal that correlated with the growth arrest (Figure 7c). The G-overhang signal was found decreased by 27% after 10 days. Therefore, these data suggested that the delayed growth arrest and apoptosis induced by

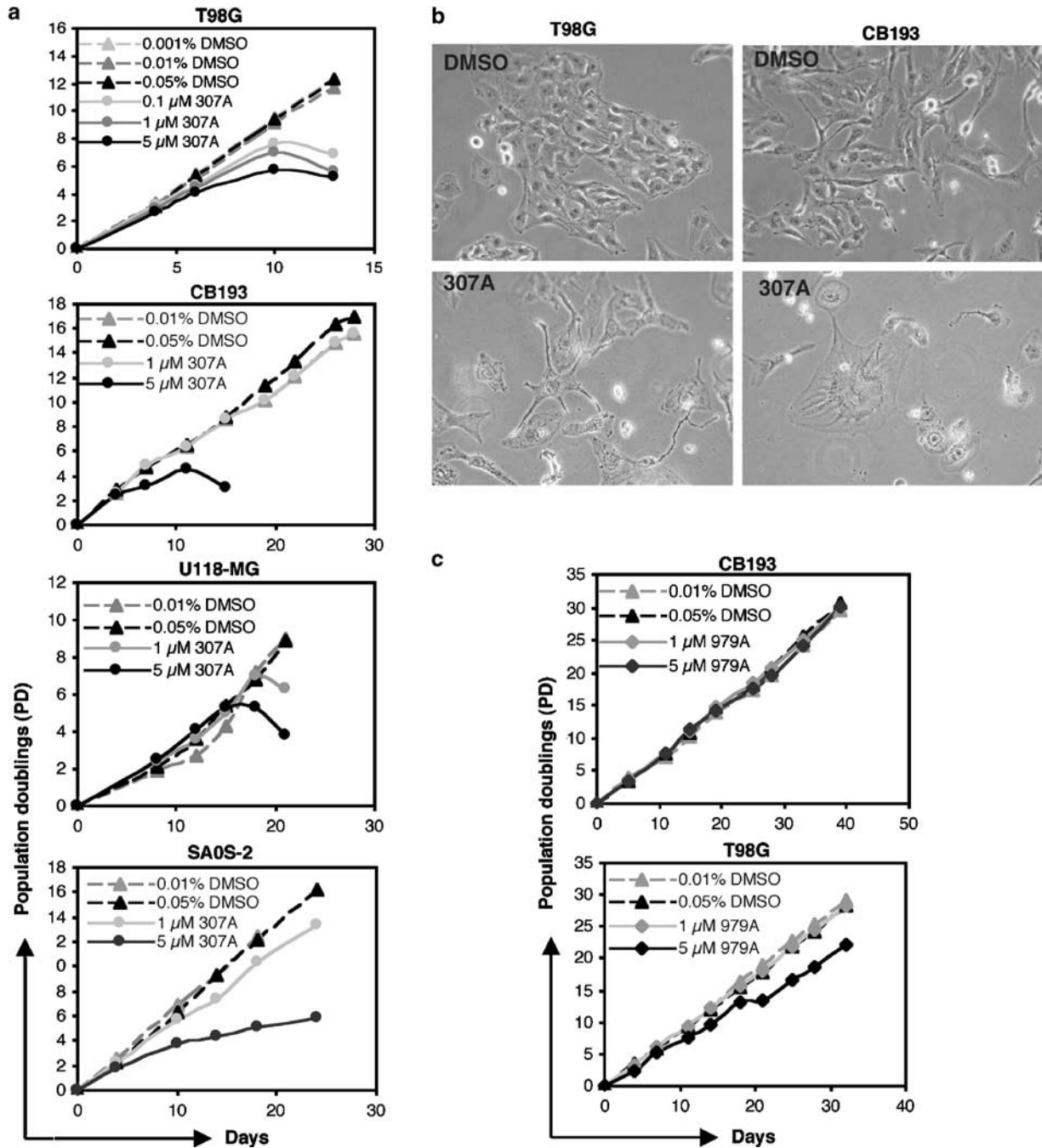


Figure 2 The pyridine derivative 307A inhibited growth in the telomerase-positive glioma and ALT cell lines. (a) Representative cell growth curves for the cell lines cultured with various concentrations of 307A or DMSO. (b) Phase-contrast micrographs showing the cellular morphology of T98G treated for 13 days with 0.001% DMSO (top-left) or with 0.1 μM 307A (bottom-left) and of CB193 cells treated for 11 days with 0.05% DMSO (top-right) or with 5 μM 307A (bottom-right). Representative images are shown (original magnification: × 10 objective). (c) Cell growth curves for CB193 and T98G cells cultured with 979A or DMSO. Similar results were obtained in two independent experiments

pyridine dicarboxamide derivatives may be related to an alteration of the length of telomeric G-overhang, but not to a modification of the telomeric double-stranded DNA length, in agreement with the previous finding on other cell lines using either a hTERT dominant-negative construct or another G-quadruplex ligand (Masutomi *et al.*, 2003; Gomez *et al.*, 2004).

Finally, we showed that 307A induced telomere instability in T98G and CB193 cultures, as evidenced by the frequent detection (Table 3) of dicentric (Figure 7d) and ring chromosomes (Figure 7e) in metaphase spreads. Moreover, anaphase bridges (Figure 7f) that are characteristic of chromosome end fusions were also frequently detected in those cultures (Counter *et al.*, 1992).

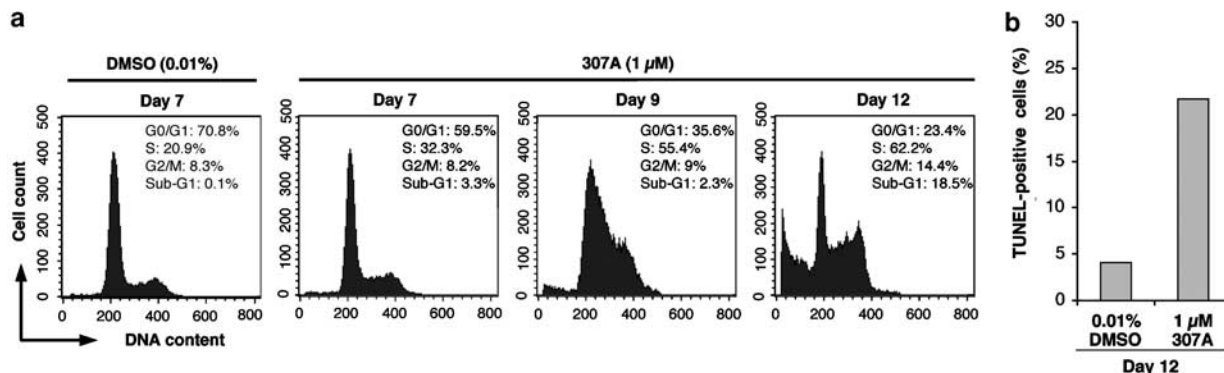


Figure 3 Cell cycle arrest and apoptosis induced by the pyridine derivative 307A in T98G glioma cells. (a) Cell cycle analysis of T98G cultures treated with 307A or DMSO. The percentages of cells in different phases of the cell cycle are expressed with respect to the total number of viable cells. The percentages of cells undergoing apoptosis (sub-G1%) are expressed with respect to the total number of cells. (b) TUNEL labeling of T98G cells treated with 1 μM 307A for 12 days or with 0.01% DMSO. Samples were analysed by flow cytometry and the proportion of TUNEL-positive cells was expressed as the percentage of the total population

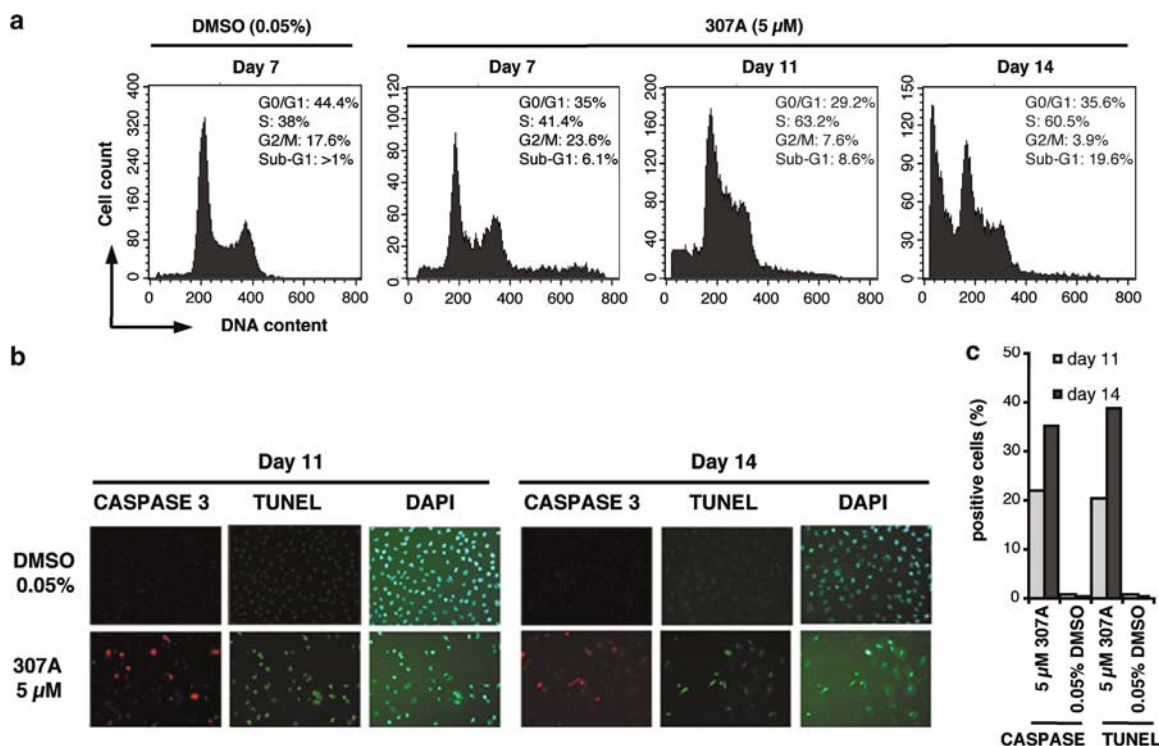


Figure 4 Cell cycle arrest, apoptosis and activation of caspase-3 induced by pyridine derivative 307A in CB193 glioma cells. (a) Cell cycle analysis of CB193 cultures treated with 307A or DMSO. The percentages of cells in different phases of the cell cycle are expressed with respect to the total number of viable cells. The percentages of cells undergoing apoptosis (sub-G1%) are expressed with respect to the total number of cells. (b) Cleaved caspase-3 detection by immunofluorescence (red) and TUNEL staining of apoptotic cells (green) in CB193 cultured with 5 μM 307A for 11 and 14 days or control cells treated with 0.05% DMSO. Nuclei were stained with DAPI (blue). Original magnification: × 20. (c) The histograms show the percentages of caspase- and TUNEL-positive cells with respect to the total DAPI-stained population

Discussion

We report here the characterization of the cellular effects of a new chemical series (pyridine derivatives) with very high specificity and selectivity toward G-quadruplex structures and telomerase inhibition. We show that four 2,6-pyridine-dicarboxamide derivatives

(831A, 832A, 307A and 360A) blocked cell proliferation and induced apoptosis, but not senescence, in cultures of three telomerase-positive glioma cell lines – T98G, CB193 and U118-MG – and in cultures of an ALT cell line. The lack of effects of 979A, a control pyridine derivative with no specific G-quadruplex affinity or telomerase inhibition capacity, highly suggests that

cellular effects of the active pyridine derivatives were specific to their affinity toward G-quadruplex structures. Moreover, the lack of effects of G-quadruplex ligands on cultures of normal astrocytes after 7 days of treatment, as assessed by WST-1 assay, suggests that telomerase-negative normal cells may be less sensitive to these compounds than immortalized cells maintaining their telomeres by means of telomerase or ALT.

The precise mechanisms of action of G-quadruplex ligands are not completely understood. G-quadruplex ligands are hypothesized to stabilize the G-quadruplex structures adopted by the 3' overhang of the telomeres, thereby preventing telomerase-mediated telomere elon-

gation (Neidle and Parkinson, 2002). The direct inhibition of telomerase has been shown to result in the gradual shortening of telomeres with successive cell divisions, until a critical length is reached, resulting in signaling for cell growth arrest and cell death (Herbert *et al.*, 1999). Selective telomerase inhibitors are therefore supposed to act only after some rounds of replication, depending on initial telomere lengths. Consistent with such a mechanism of action, we showed that active pyridine derivatives required several rounds of replication (3–7 depending on the cell line) to induce cell growth arrest even when these compounds were used at high concentrations. Moreover, the active pyridine derivatives induced cell death in the glioma cell lines within delays (1–3 weeks depending on drug concentration) similar to that observed by direct inhibition of telomerase activity in cell lines with short telomeres in other studies (Hahn *et al.*, 1999; Zhang *et al.*, 1999; Nakajima *et al.*, 2003).

The frequent detection of both chromosome end fusions in metaphasic nuclei and anaphase bridges confirmed that pyridine derivatives act on telomeres and induce telomeric instability as in the case of deprotected telomeres (van Steensel *et al.*, 1998; De Lange, 2002). However, we did not detect telomere shortening in cultures exposed to pyridine derivatives. In particular, telomere lengths were similar in treated T98G and CB193 cells at the time of cell growth arrest and just before cell death. Although it could not be excluded that treatments may have caused slight telomere erosion due to telomerase inhibition sufficient (especially for the shortest telomeres) to cause cell growth arrest, our data suggest that whole telomere

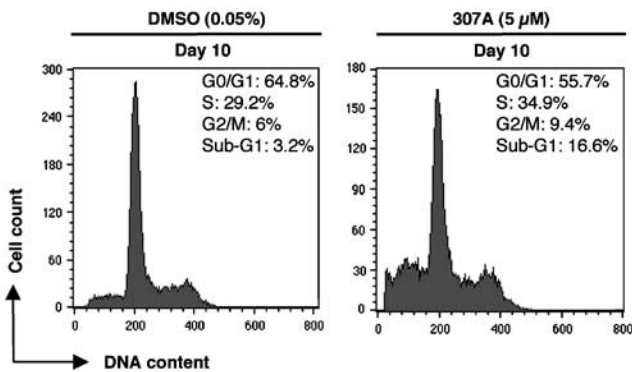


Figure 5 Apoptosis induced by the pyridine derivative 307A in the ALT cell line, SAOS-2. Cell cycle analysis of SAOS-2 cultures treated with 307A or DMSO. The percentages of cells in different phases of the cell cycle are expressed with respect to the total number of viable cells. The percentages of cells undergoing apoptosis (sub-G1%) are expressed with respect to the total number of cells

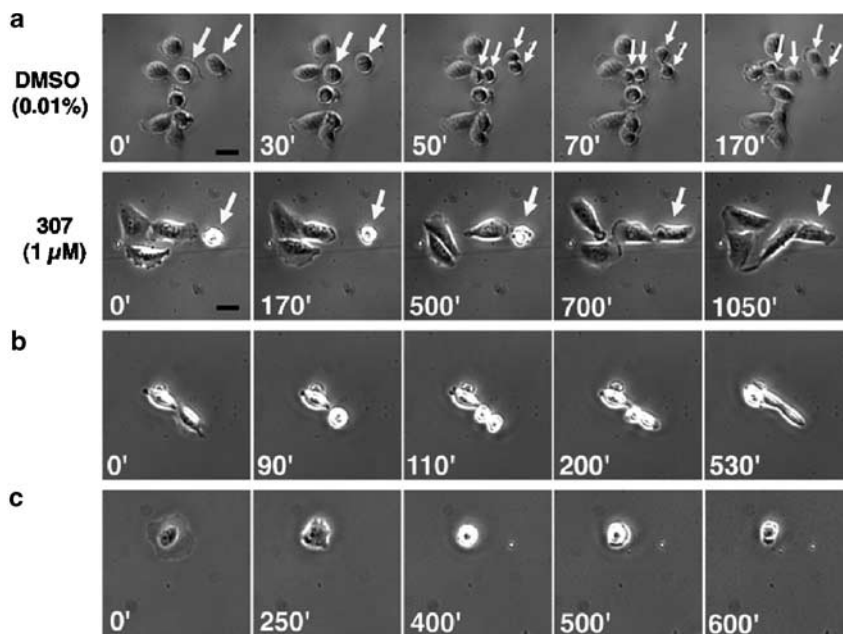


Figure 6 Time-lapse video live-cell imaging of T98G cell line treated for 7 days with 1 μM 307A. (a) The duration of normal cell division is about 200 min (DMSO 0.01%; upper row), whereas some cells in pyridine derivative-treated cultures remained arrested in metaphase for more than 500 min (lower row). Large arrows indicate cells undergoing mitosis and little arrows indicate daughter cells. In treated cultures, mitotic cells also exhibited defaults of cytokinesis (b), whereas other cells died during mitosis (c). Scale bar, 50 μm (see Supplemental movies S1, S2, S3 and S4)

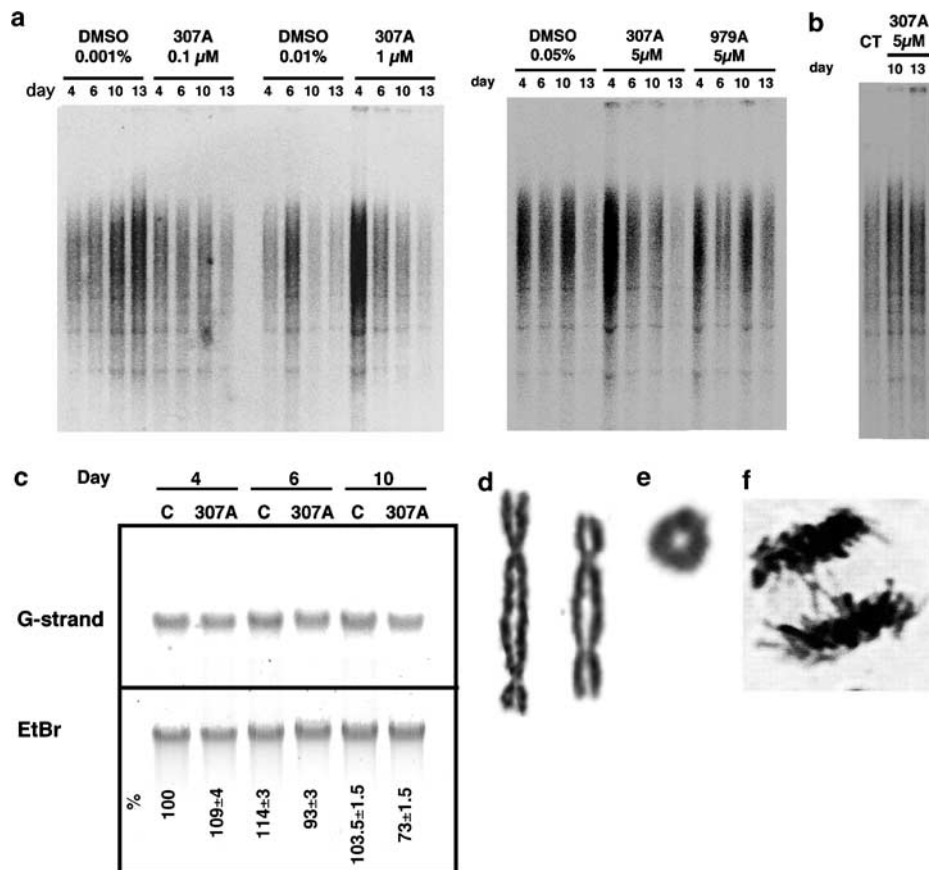


Figure 7 Shortening of the telomeric 3'-overhang and telomeric instability induced by pyridine derivatives in glioma cell lines. (a) TRF length analysis for T98G cells treated with various concentrations of DMSO, 307A or 979A for 4, 6, 10 and 13 days, showing lack of evidence of telomere shortening. (b) TRF length analysis for CB193 cells treated with DMSO (CT) or 307A, showing lack of evidence of telomere shortening. (c) Nondenaturing solution hybridization analysis of the 3' telomeric overhang in T98G cells treated either with 307A (1 μ M) or with 0.01% DMSO (C) for 4, 6 and 10 days, respectively. G-strand: hybridization signal of the gel with 21C probe. EtBr: ethidium bromide staining of the gel. Values at the bottom indicate the relative G-strand overhang signal, normalized to the EtBr signal and expressed as the relative hybridization of the 21C probe from untreated T98G DNA defined as 100%. Values are the means of two independent determinations (\pm s.d.). (d, e) Typical dicentric chromosomes (d) and ring chromosome (e) found in the metaphase spread of T98G cells after 10 days of treatment by 307A. (f) Representative image of anaphase bridges induced by 307A in T98G cells after 10 days of treatment. DNA was stained by Giemsa (original magnification: \times 100 objective)

Table 3 Induction of chromosome end-to-end associations by 307A in T98G and CB193 glioma cells at day 10

Cell line	T98G		CB193	
	DMSO (0.01%)	307A (1 μ M)	DMSO (0.05%)	307A (5 μ M)
Number of metaphases examined	195	121	131	201
Fraction with dicentric chromosome (%)	6	55	5	36
Fraction with ring chromosome (%)	0	4	0	2

shortening is not the main mechanism induced by pyridine derivatives leading to telomeric instability. This is also supported by the observation that telomerase-positive lymphoblastic cells, CEM1301, that have very long telomeres (mean TRF greater than 30 kb) undergo apoptosis in response to the G-quadruplex ligands with kinetics similar to that of glioma cell lines with short telomeres (Granotier *et al.*, submitted).

Telomeric G-overhang degradation was found to be associated with the onset of replicative senescence in

normal cultured cells (Stewart *et al.*, 2003), but also with telomere capping alterations when the function of TRF2 was inactivated (van Steensel *et al.*, 1998). A recent work also indicated that telomestatin induced G-overhang degradation (38–52% in human A549 cells treated for 8–12 days) in association with the onset of replicative senescence (Gomez *et al.*, 2004). We observed a slight, but significant, shortening of single-stranded 3' overhang in T98G cells treated by 307A. This shortening of the 3' overhang might have resulted either from

inhibition of telomerase-mediated telomere maintenance or from perturbations of the end-capping functions of other proteins, such as hPOT1 (Baumann and Cech, 2001). Alternatively, it could have resulted from attempts of the cellular machinery to eliminate G-quadruplex structures and their ligands through endonuclease-mediated degradation (Zhu *et al.*, 2003). However, further experiments are needed to determine: (1) if the 3' overhang shortening is a general phenomenon in cells treated with G-quadruplex ligands or is limited to certain cell types such as A549 (Gomez *et al.*, 2004) and T98G cells (this study) and (2) if 3' overhang shortening is the main cause of telomeric instability in G-quadruplex-treated cells or only a secondary consequence of the treatment (for example, related to apoptotic pathways). Indeed, it could not be ruled out that telomeric instability may be directly due to other mechanisms such as the perturbation of the correct conformation of telomere ends by G-quadruplex stabilization.

We showed that S-phase arrest preceded the induction of apoptosis by 307A in glioma cell lines, suggesting activation of the S-phase DNA damage checkpoint. Since pyridine derivatives, in contrast to nucleoside analogs (Shi *et al.*, 2001; Sampath *et al.*, 2002), require at least three to five cell divisions to elicit S-phase arrest, they are unlikely to block DNA replication nonspecifically. Rather, these data may be related to those of Eller *et al.* (2003) showing that DNA oligonucleotides homologous to the telomere 3' overhang sequence specifically activate an S-phase checkpoint by modifying Nijmegen breakage syndrome protein (p95/NBS1), a response mediated in part by ATM but independent of p53. Moreover, the involvement of ATM-dependent DNA damage response in the activity of another G-quadruplex-interactive telomerase inhibitor has been reported previously (Tsuchi *et al.*, 2003). Such a pathway could therefore be involved in the cellular effects of the pyridine derivatives. The shortening of the telomere 3' overhangs induced by the G-quadruplex ligands could disrupt the normal telomere loop structure, and thus result in their abnormal exposure leading to a cellular DNA damage response that could involve p95/NBS1 and ATM, but not p53, since T98G is mutated for p53 (Mercer *et al.*, 1990). Apoptosis of glioma cells could thus result from the inability of cells to pass S-phase checkpoints, but also from alterations during mitosis for cells that pass this checkpoint and progress in the cell cycle.

The dramatic increase of metaphase duration and the defects in cytokinesis in treated cultures are probably the direct consequence of telomere instability that allows chromosome end fusions and thus prevents the correct segregation of telomeres. Recently, Dynek and Smith (2004) have demonstrated that telomeres of sister chromatids normally associate and that their resolution is required for progression through mitosis. G-quadruplex ligands could thus also interfere with these steps by prevention of the correct conformation of telomeres and/or by inducing the formation of intermolecular G-

quadruplex structures possibly favored by sister chromatid association.

Other compounds interacting with G-quadruplex structures, such as the pentacyclic acridine RHPS4 (Gowan *et al.*, 2001), triazine derivatives (Riou *et al.*, 2002) and a fluoroquinoanthroxazine series (Kim *et al.*, 2003), have been shown to inhibit proliferation in ALT cell lines. We showed that the pyridine derivatives alter cell cycle progression and induced apoptosis of SAOS-2 cells, but not exactly in the same ways as those in glioma cell lines. The effects of our pyridine derivatives on ALT cell lines may be also related to impairment of telomere functions, as proposed for telomerase-positive cell lines. Alternatively, the inhibition of specific helicases involved in ALT may have impaired homologous recombination, resulting in cell growth arrest and ALT cell death as reported for other G4-interactive ligands (Li *et al.*, 2001).

As we show here, the effects of G4-interactive ligands depend on the cellular context. The lack of induction of a senescence program in glioma cell lines and in SAOS-2 cells may be related to the defects in essential genes, for example, T98G and U118-MG have no functional p53 and p16INK4A (Alonso *et al.*, 2003), whereas SAOS-2 lack both p53 and pRB (Shew *et al.*, 1990; Craig *et al.*, 1998). Defects in the induction of a senescence program may allow cells to continue to divide despite G-quadruplex-induced telomere dysfunctions, a process leading to the induction apoptotic pathway as a consequence of multiple cell cycle alterations.

We show here that the new highly selective G-quadruplex ligands of a 2,6-pyridine-dicarboxamide series inhibited proliferation and induced apoptosis of telomerase-positive glioma cell lines with short telomeres and were also effective on ALT cell lines. They interfere with telomere maintenance and multiple steps of the cell cycle. They represent thus a promising new family of compounds for use in cancer therapy. Alone, or in combination with other treatments, such as radiotherapy, they may provide a new basis for the treatment of glioblastoma multiforme, which currently has a very poor prognosis, but also of other types of telomerase-positive or ALT tumor.

Materials and methods

Cells

Human glioma T98G, CB193 and U118-MG cells were kindly provided by Dr Gras (CEA, France) and primary cultures of normal human astrocytes by Dr Horellou (INSERM EMI 0020, Clamart, France). Human osteosarcoma cell line SAOS-2 was obtained from Dr Malfroy (Institut Curie, France). Cultures were performed in DMEM medium (Invitrogen) supplemented with 10% fetal bovine serum (Invitrogen), 2 mM glutamine (Sigma) and antibiotics (penicillin, 100 U/ml; streptomycin, 100 µg/ml).

Chemical compounds

Triazine derivative 115405 was synthesized according to patent WO 0140218. Derivatives 831A, 832A, 307A, 979A and 360A

have been described elsewhere (Mailliet *et al.*, 2003; Lemarteleur *et al.*, 2004) and their detailed chemical synthesis will be presented in another paper. These compounds were dissolved in dimethyl sulfoxide (DMSO) at a concentration of 10 mM to produce stock solutions, which were stored at -20°C . These solutions were diluted with culture medium immediately before use.

Cell treatments

The cell proliferation reagent WST-1 assay (Roche) was performed according to manufacturer's instructions. In brief, cells were seeded at various densities, depending on cell type ($0.25\text{--}4 \times 10^3$ cells/well in $100\ \mu\text{l}$ complete medium), in 96-well culture plates and treated with various concentrations ($0.1\text{--}20\ \mu\text{M}$) of compounds or the corresponding concentrations of DMSO (control wells) for 3 or 7 days at 37°C in an atmosphere containing 5% CO_2 . For 7-day assays, the medium was changed on day 3. Experiments were performed in triplicate.

For long-term exposure studies, cells were grown in $75\ \text{cm}^2$ flasks (5×10^5 cells/flask) and exposed to compounds at various concentrations. Control cells were treated with the corresponding concentrations of DMSO. Every 3–4 days, cells were treated with trypsin, and counted using trypan blue. We then reseeded flasks at a density of 5×10^5 cells/flask. The remaining cells were collected for further analysis. Experiments were performed at least in duplicate.

Telomerase activity assay

Telomerase activity was assessed with the TRAPeze ELISA Telomerase Detection Kit (Intergen) according to the manufacturer's instructions. Briefly, we assayed 100 ng of protein extract in a $50\ \mu\text{l}$ reaction mixture containing $10\ \mu\text{l}$ of $5 \times$ TRAP reaction mix and 2 U of Taq DNA polymerase (Amersham Pharmacia Biotech). The reaction mixture was incubated for 30 min at 30°C for telomerase extension, and was then subjected to PCR amplification for 33 cycles of 94°C for 30 s, and 55°C for 30 s on a PTC-200 thermocycler (MJ Research). Amplified products were visualized on a 12.5% nondenaturing polyacrylamide gel, after electrophoresis and staining with ethidium bromide.

Semiquantitative analysis of hTERT gene expression by Light-Cycler PCR

Reverse transcription was performed with $3\ \mu\text{g}$ of total RNA. The first-strand cDNA was synthesized with $0.75\ \mu\text{g}$ of random hexamers (Promega) and 300 U of Moloney murine leukemia virus reverse transcriptase (Invitrogen). Amplification was performed in $8\ \mu\text{l}$ of Light Cycler DNA master SYBR Green I mix (Roche) containing 3 mM MgCl_2 , $2\ \mu\text{l}$ of cDNA and primers specific for hTERT ($5'$ -TGGCACGGCTTTTGTT-CAGA-3' and $5'$ -CTTGGCTTTCAGGATGGAGT-3'). The level of hTERT transcripts was normalized by simultaneously amplifying the human 18S rRNA transcript, as a control, with the specific primers ($5'$ -TGTGATGCCCTTAGATGTCC-3' and $5'$ -CTTATGACCCGCACTTACTG-3'). Serial dilutions ($1\text{--}10^{-4}$) of a control cDNA sample (obtained from CEM 1301) were also used as external standards in each run. Amplifications were performed by 45 cycles of a three-step PCR in a Light Cycler (Roche): 95°C for 10 s, 57°C for 10 s and 72°C for 8 s for 18S rRNA and 95°C for 10 s, 60°C for 10 s and 72°C for 10 s for hTERT, with fluorescence detection after each cycle. After the final cycle, melting-point analysis at temperatures of $70\text{--}95^{\circ}\text{C}$ was performed for all samples, to assess the specificity of amplification. The hTERT/18S rRNA

transcript ratio was calculated for each sample and hTERT mRNA levels were expressed with respect to the control.

Cell cycle analysis

Cells ($0.5\text{--}1 \times 10^6$) were washed with PBS, fixed in 70% ethanol and kept at -20°C for at least 24 h. They were then washed in PBS and resuspended in $50\ \mu\text{g}/\text{ml}$ propidium iodide and RNase ($10\ \mu\text{g}/\text{ml}$) in PBS. The cell suspension was incubated for 30 min at room temperature and cell cycle distribution was determined by flow cytometry (FACS-Calibur, Becton-Dickinson), with CellQuest software analysis and quantification using ModFit software.

TUNEL assay

Apoptotic cells were quantified by TUNEL assay, using the *In situ* Cell Death Detection Kit Fluorescein (Roche) according to the manufacturer's instructions. Cell preparations for microscopy were washed and counterstained with DAPI before observation under a fluorescence microscope (Olympus BX51). The percentage of cells that were apoptotic was calculated from at least 200 cells per sample. For flow cytometry analysis, cells were washed, resuspended in $5\ \mu\text{g}/\text{ml}$ of propidium iodide in PBS and then subjected to flow cytometry.

Detection of cleaved caspase-3

Cells were fixed in 4% paraformaldehyde, and permeabilized using 0.1% Triton-X100. They were then incubated with a 1:200 dilution of rabbit antibody specific for the cleaved form of caspase-3 (cleaved caspase-3 (Asp175) antibody, Cell Signaling) for 50 min at room temperature. After washings, cells were incubated with a 1:100 dilution of Alexa Fluor 594-conjugated anti-rabbit IgG (Molecular Probes) for 1 h at room temperature and then counterstained with DAPI before observation under a fluorescence microscope.

Time-lapse video microscopy

The microscopy setup included an inverted microscope (Olympus IX81) coupled with a coolsnap HQ camera (Princeton town instrument), which were controlled by Metamorph 6.2.1 software (Universal Imaging Corp.). During acquisition, cells were placed in an incubator chamber (LIS) at 37°C . Phase-contrast images were taken using a CplanFI $\times 10/0.3$ objective with 30 ms exposure time, every 10 min during 18 h. All phase-contrast pictures were converted to eight-bit files before being assembled. Movies were processed in AVI format with Metamorph software.

Telomere length analysis

Telomere length was assessed by Southern blot determination of the mean TRF length as previously described (Pommier *et al.*, 1997). Briefly, high-molecular weight genomic DNA was digested with *HinfI* (10 U). Digested DNA ($3\text{--}8\ \mu\text{g}/\text{well}$) was separated by electrophoresis (50 V for 14 h) in a 0.5 or 1% agarose gel, transferred to a nylon membrane (Hybond N+, Amersham Pharmacia Biotech). Hybridization was carried out with a ^{32}P -end-labeled probe, $(\text{CCCTAA})_4$, for 16 h at 42°C . Membranes were washed and placed against Molecular Imager screens overnight. The results were then analysed with Molecular Analysis 2.1 and Profit softwares.

Analysis of the telomeric-3' overhang

The non-denaturing hybridization assay to detect 3' telomere G-overhang was performed with a modification of the procedure described previously (Cimino-Reale *et al.*, 2001; Gomez *et al.*, 2003). Aliquots of 2.5 µg of undigested genomic DNA were hybridized at 50°C overnight with 0.5 pmol of γ -³²P-ATP-labeled 21C oligonucleotide (5'-CCCTAACCC-TAACCCCTAACCC-3') in Na/Mg hybridization buffer containing 20 mM Tris, pH 8.0, 0.5 mM EDTA, 50 mM NaCl, 10 mM MgCl₂ in a volume of 20 µl. Reactions were stopped by the addition of 6 µl of loading buffer (20% glycerol, 1 mM EDTA and 0.2% bromophenol blue) and samples were size-fractionated on 0.8% agarose gels in 1× TBE buffer containing ethidium bromide (EtBr). Gels were dried on a Whatman filter paper. EtBr fluorescence and radioactivity were scanned with a phosphorimager (Typhoon 9210, Amersham). Results were expressed as the relative hybridization signal normalized to the fluorescent signal of EtBr.

References

Alonso M, Tamasdan C, Miller DC and Newcomb EW. (2003). *Mol. Cancer Ther.*, **2**, 139–150.
 Baumann P and Cech TR. (2001). *Science*, **292**, 1171–1175.
 Bryan TM, Englezou A, Dalla-Pozza L, Dunham MA and Reddel RR. (1997). *Nat. Med.*, **3**, 1271–1274.
 Chan SW and Blackburn EH. (2002). *Oncogene*, **21**, 553–563.
 Cimino-Reale G, Pascale E, Battiloro E, Starace G, Verna R and D'Ambrosio E. (2001). *Nucleic Acids Res.*, **29**, E35.
 Counter CM, Avilion AA, LeFeuvre CE, Stewart NG, Greider CW, Harley CB and Bacchetti S. (1992). *EMBO J.*, **11**, 1919–1921.
 Craig C, Kim M, Ohri E, Wersto R, Katayose D, Li Z, Choi YH, Mudahar B, Srivastava S, Seth P and Cowan K. (1998). *Oncogene*, **16**, 265–272.
 De Lange T. (2002). *Oncogene*, **21**, 532–540.
 Dutrillaux B and Couturier J. (1981). *La pratique de l'analyse chromosomique*. Masson (ed). IRL Press: Paris.
 Dynek JN and Smith S. (2004). *Science*, **304**, 97–100.
 Eller MS, Li GZ, Firoozabadi R, Puri N and Gilchrist BA. (2003). *Faseb J.*, **17**, 152–162.
 Gomez D, Aouali N, Renaud A, Douarre C, Shin-ya K, Tazi J, Martinez S, Trentesaux C, Morjani H and Riou JF. (2003). *Cancer Res.*, **63**, 6149–6153.
 Gomez D, Mergny JL and Riou JF. (2002). *Cancer Res.*, **62**, 3365–3368.
 Gomez D, Paterski R, Lemarteleur T, Shin-Ya K, Mergny JL and Riou JF. (2004). *J. Biol. Chem.*, **279**, 41487–41494.
 Gowan SM, Harrison JR, Patterson L, Valenti M, Read MA, Neidle S and Kelland LR. (2002). *Mol. Pharmacol.*, **61**, 1154–1162.
 Gowan SM, Heald R, Stevens MF and Kelland LR. (2001). *Mol. Pharmacol.*, **60**, 981–988.
 Hahn WC, Stewart SA, Brooks MW, York SG, Eaton E, Kurachi A, Beijersbergen RL, Knoll JH, Meyerson M and Weinberg RA. (1999). *Nat. Med.*, **5**, 1164–1170.
 Hakin-Smith V, Jellinek DA, Levy D, Carroll T, Teo M, Timperley WR, McKay MJ, Reddel RR and Royds JA. (2003). *Lancet*, **361**, 836–838.
 Henson JD, Neumann AA, Yeager TR and Reddel RR. (2002). *Oncogene*, **21**, 598–610.
 Herbert B, Pitts AE, Baker SI, Hamilton SE, Wright WE, Shay JW and Corey DR. (1999). *Proc. Natl. Acad. Sci. USA*, **96**, 14276–14281.
 Holland EC. (2000). *Proc. Natl. Acad. Sci. USA*, **97**, 6242–6244.

Chromosome analysis in metaphase and anaphase cells

Metaphase spreads of glioma cells were prepared as previously described (Dutrillaux and Couturier, 1981) and counterstained with Giemsa. Anaphase cells were visualized by giemsa staining of T98G or CB193 cells grown in 8-chambers labteks (Nunc) in the presence of 307A or DMSO during 10 days and fixed with 4% formaldehyde.

Acknowledgements

We thank A Boistard, E Goodall, O Etienne, E Nowak, P Millet, C Silva Lages (CEA, Fontenay-aux-Roses, France), L Guittat and L Lacroix (MNHN, Paris, France) for technical support and helpful discussions. This work was supported by an *Action Concertée Incitative 'Molécules et Cibles Thérapeutiques'* grant from the French Ministry of Research and an *Association pour la recherche sur le Cancer* grant (grant 3365 to J-L M and grant 4691 to J-F R).

Kim MY, Duan W, Gleason-Guzman M and Hurley LH. (2003). *J. Med. Chem.*, **46**, 571–583.
 Lemarteleur T, Gomez D, Paterski R, Mandine E, Mailliet P and Riou JF. (2004). *Biochem. Biophys. Res. Commun.*, **323**, 802–808.
 Li JL, Harrison RJ, Reszka AP, Brosh RMJ, Bohr VA, Neidle S and Hickson ID. (2001). *Biochemistry*, **40**, 15194–15202.
 Mailliet P, De Lomos E, Caulfield T, Mandine E, Petitgenet O, Renou E, Belmokhtar C, Mergny JL, Guittat L, Gomez D and Riou JF. (2003). *94th AACR Meeting* LB28. July 11–14, Washington DC, USA.
 Masutomi K, Yu EY, Khurts S, Ben-Porath I, Currier JL, Metz GB, Brooks MW, Kaneko S, Murakami S, DeCaprio JA, Weinberg RA, Stewart SA and Hahn WC. (2003). *Cell*, **114**, 241–253.
 McEachern MJ, Krauskopf A and Blackburn EH. (2000). *Annu. Rev. Genet.*, **34**, 331–358.
 Mercer WE, Shields MT, Amin M, Sauve GJ, Appella E, Romano JW and Ullrich SJ. (1990). *Proc. Natl. Acad. Sci. USA*, **87**, 6166–6170.
 Mergny JL, Riou JF, Mailliet P, Teulade-Fichou MP and Gilson E. (2002). *Nucleic Acids Res.*, **30**, 839–865.
 Nakajima A, Tauchi T, Sashida G, Sumi M, Abe K, Yamamoto K, Ohyashiki JH and Ohyashiki K. (2003). *Leukemia*, **17**, 560–567.
 Neidle S and Parkinson G. (2002). *Nat. Rev. Drug Discov.*, **1**, 383–393.
 Neidle S and Parkinson GN. (2003). *Curr. Opin. Struct. Biol.*, **13**, 275–283.
 Pommier JP, Gauthier L, Livartowski J, Galanaud P, Boue F, Dulioust A, Marce D, Ducray C, Sabatier L, Lebeau J and Boussin FD. (1997). *Virology*, **231**, 148–154.
 Riou JF, Guittat L, Mailliet P, Laoui A, Renou E, Petitgenet O, Megnin-Chanet F, Hélène C and Mergny JL. (2002). *Proc. Natl. Acad. Sci. USA*, **99**, 2672–2677.
 Sampath D, Shi Z and Plunkett W. (2002). *Mol. Pharmacol.*, **62**, 680–688.
 Shammass MA, Shmookler Reis RJ, Akiyama M, Koley H, Chauhan D, Hideshima T, Goyal RK, Hurley LH, Anderson KC and Munshi NC. (2003). *Mol. Cancer Ther.*, **2**, 825–833.
 Shay JW and Bacchetti S. (1997). *Eur. J. Cancer*, **33**, 787–791.
 Shew JY, Lin BT, Chen PL, Tseng BY, Yang-Feng TL and Lee WH. (1990). *Proc. Natl. Acad. Sci. USA*, **87**, 6–10.

- Shi Z, Azuma A, Sampath D, Li YX, Huang P and Plunkett W. (2001). *Cancer Res.*, **61**, 1065–1072.
- Stewart SA, Ben-Porath I, Carey VJ, O'Connor BF, Hahn WC and Weinberg RA. (2003). *Nat. Genet.*, **33**, 492–496.
- Tauchi T, Shin-Ya K, Sashida G, Sumi M, Nakajima A, Shimamoto T, Ohyashiki JH and Ohyashiki K. (2003). *Oncogene*, **22**, 5338–5347.
- van Steensel B, Smogorzewska A and de Lange T. (1998). *Cell*, **92**, 401–413.
- Zahler AM, Williamson JR, Cech TR and Prescott DM. (1991). *Nature*, **350**, 718–720.
- Zhang X, Mar V, Zhou W, Harrington L and Robinson MO. (1999). *Genes Dev.*, **13**, 2388–2399.
- Zhu XD, Niedernhofer L, Kuster B, Mann M, Hoeijmakers JH and de Lange T. (2003). *Mol. Cell*, **12**, 1489–1498.

Supplementary Information accompanies the paper on Oncogene website (<http://www.nature.com/onc>)